FEBS Letters 587 (2013) 128–135

ELSEVIER

FEBS Letters

journal homepage: www.FEBSLetters.org

PDT-induced HSP70 externalization up-regulates NO production via TLR2 signal pathway in macrophages

Sheng Song [a], Feifan Zhou [a], Wei R. Chen [a,b], Da Xing [a,*]

[a] MOE Key Laboratory of Laser Life Science & Institute of Laser Life Science, College of Biophotonics, South China Normal University, Guangzhou 510631, China
[b] Biomedical Engineering Program, Department of Engineering and Physics, University of Central Oklahoma, Edmond, Oklahoma 73034, USA

ARTICLE INFO

Article history:
Received 28 July 2012
Revised 31 October 2012
Accepted 16 November 2012
Available online 14 December 2012

Edited by Laszlo Nagy

Keywords:
Apoptotic cell
HSP70
Innate immune
NO
Phagocytosis
TLRs

ABSTRACT

We studied the molecular mechanism underlying PDT-induced apoptosis-dependent macrophage activation, particularly through NO production. We demonstrate that NO production is initially induced by HSP70 on the apoptotic cell surface, and is further enhanced by macrophage phagocytosis. Additionally, we found that apoptotic cells, through TLR2, could activate PI3K, and this could be either dependent or independent of the activation of MyD88. These results reveal a novel pathway linking innate immune signalling to apoptotic cells and point at HSP70 as an important antitumor immunostimulant. They also indicate that PDT-induced apoptosis has an important role in macrophage innate immunity.

Structured summary of protein interactions:
p85α and MyD88 physically interact by fluorescent resonance energy transfer (View interaction)
TLR2 and p85α physically interact by fluorescent resonance energy transfer (View interaction).

1. Introduction

Considerable data support the idea that apoptotic cells (ACs) participate in immune response, but its immunological mechanism is still unclear [1,2]. Although engulfment of ACs has traditionally been regarded as being immunologically suppressive, recent studies have suggested that infected ACs are a critical component of the innate immune signals [3].

The ideal cancer treatment modalities should not only cause tumor regression and eradication, but also induce a systemic antitumor immunity. Photodynamic therapy (PDT) is a relatively new modality for the clinical treatment of cancer. In addition, PDT has shown antitumor effects in regulating the host immune systems [4–7]. Since macrophages exist in most tumor sites and are the most abundant infiltrating cells in tumors, macrophage-targeted PDT has been applied in the selective killing of cells involved in inflammation and tumor [8]. Macrophages are classified as M1 and M2. M1 macrophages promote anti-tumour immunity while M2 macrophages derail it [9]. Mounting evidence shows a more complex progress of macrophage activation during PDT, which performs distinct immunological functions and different physiologies on surrounding cells and tissues [10,11]. Studies have demonstrated that activated macrophages not only can distinguish tumor cells from normal host cells, but also are capable of reducing tumor cell growth and achieving tumor cytotoxicity without the aid of specific antibodies [12]. In addition, accumulating evidence shows that the apoptotic rather than necrotic tumor cells induce a potent immune response [13]. We also demonstrated that TLR2 initiated such signalling cascades in response to PDT-induced AC [14]. It is known that the released endogenous molecules of necrotic cells are recognized as danger signals. Recent evidence has also shown that PDT-induced AC is associated with danger signals that can activate innate immune cells [15].

Since macrophages produce a large volume of ROS (reactive oxygen species) through respiratory burst, nitric oxide (NO) release has been a sign of respiratory burst. The high-output of NO and the over-expressed inducible nitric oxide synthase (iNOS) are considered as "activated macrophage marker". Macrophages can kill tumor cells by releasing high levels of NO and related reactive nitrogen species such as nitroxyl and peroxynitrite, after up-regulation of expression of the iNOS gene [16]. Importantly, as an agent of inflammation and cell-mediated immunity, iNOS-derived NO also plays an important role in host anti-tumor immunities [17]. Since the NO production

Abbreviations: AC, apoptotic cell; CFP, cyan fluorescent protein; CM, conditioned medium; Cyt B, cytochalasin B; DN MyD88, dominant negative myeloid differentiation factor-88; DN TLR2, dominant negative TLR2; FRET, fluorescence resonance energy transfer; GFP, green fluorescent protein; HSPs, heat shock proteins; iNOS, inducible nitric oxide synthase; NC, necrotic cells; NF-κB, nuclear factor κB; NO, nitric oxide; PDT, photodynamic therapy; shRNA, short hairpin RNA; TLR, toll like receptor; YFP, yellow fluorescent protein

* Corresponding author. Fax: +86 20 85216052.
E-mail address: xingda@scnu.edu.cn (D. Xing).

0014-5793/$36.00 © 2012 Federation of European Biochemical Societies. Published by Elsevier B.V. All rights reserved.
http://dx.doi.org/10.1016/j.febslet.2012.11.026

is mainly derived from M1 macrophages, it is important to determine in the future whether M1/M2 macrophage ratio has significant implications after PDT-treated AC stimulation.

We have previously reported that cytoplasmic heat shock protein 70 (HSP70) could translocate onto the outer surface of ACs after PDT treatment [18]. In the current study, we investigated the mechanism of macrophage activation induced by PDT-treated AC, particularly through NO production. Moreover, the effects of HSP70 translocation onto tumor cell surface and the molecular mechanisms by which macrophages activation is induced by PDT-treated AC, lead to the consequent cellular responses, were also studied.

2. Materials and methods

2.1. Chemicals and plasmids

We used antibodies against iNOS, β-actin (Santa Cruz), pan-Cadherin (Abcam), HSP70 and isotype-matched control anti-HSP70 antibody (Sigma–Aldrich).

The plasmid of CFP-TLR2 was kindly supplied by Dr. Robert W. Finberg (University of Massachusetts Medical School). GFP-MyD88 was kindly supplied by Dr. Hermann Wagner (RWTH Aachen University). Dominant negative MyD88 was a gift from Dr. Ken-ichi Tanamoto (Musashino University). The dominant-negative PI3K construct Δp85α (encompasses a deletion mutant bovine p85 that lacks a binding site for the p110 catalytic subunit of PI3K) was kindly provided by Dr. Geoffrey M. Cooper of Boston University. YFP-p85α was kindly supplied by Dr. Georges Bismuth of University Paris Descartes. YFP-HSP70 was kindly supplied by Dr. Richard I. Morimoto of Northwestern University. HSP70 short hairpin RNA (shRNA) and non-target shRNA were provided by Dr. Tolkovsky and were used as previously described [19]. pNF-κB-Luc was kindly provided by Dr. X. Shen (Institute of Biophysics, Chinese Academy of Sciences). iNOS-Luc was kindly provided by Dr. David A. Geller (University of Pittsburgh School of Medicine). Dominant negative TLR2 was purchased from InvivoGen. pRL-TK was purchased from Promega.

2.2. Cell culture

Murine mammary tumor line EMT6 was maintained in RPMI 1640 medium (GIBCO), murine macrophage-like cell line RAW264.7 was maintained in Dulbecco's modified Eagle's medium (GIBCO), with 15% fetal calf serum, penicillin (100 units/ml), and streptomycin (100 μg/ml) in 5% CO_2 at 37 °C in a humidified incubator.

Mouse peritoneal macrophages were obtained as previously described [14].

2.3. Photodynamic therapy treatment of tumor cells

ACs were generated by PDT with a Photofrin (Sinclair Pharmaceuticals) dose of 10 μg/ml and a light dose of 5 J/cm^2 (10 mW/cm^2), as previously described [14]. Briefly, cells were administrated with 10 μg/ml Photofrin, then incubated in a dark, humidified atmosphere of 5% CO_2 at 37 °C for 12 h, rinsed with PBS, and exposed to light of 5 J/cm^2 (10 mW/cm^2), which resulted in more than 90% apoptotic cells. To generate ACs with overexpression HSP70 (HSP70-AC), EMT6 cells were transfected with YFP-HSP70 and G418-resistant cells were collected for PDT treatment. To generate necrotic cells (NCs), tumor cells were heated to 41 °C for 5 min and then placed in −20 °C for 30 min. The process was repeated three times. In all experiments, the ratio of apoptotic or necrotic cells to macrophages was kept at 5:1. Unless stated otherwise, ACs in the figures are PDT-induced ACs.

The AC conditioned medium (CM) was obtained by incubating 2.5×10^6 ACs in 1 ml of medium. After 2 h, cells were centrifuged for 10 min at 1000*g*. The supernatant was removed and filtered through a 0.2-μm cellulose syringe filter. The filtrate was taken as CM. When using CM, full medium was removed and replaced with CM.

2.4. Transient transfection and luciferase activity

Transient transfection of cells was performed using FuGENE HD transfection reagent (Roche) following the manufacturer's instructions. For pNF-κB or iNOS reporter luciferase activity assay, pRL-TK was used as an internal control of transfection efficiency. The ratio of luciferase activity to pRL-TK activity in each sample served as a measure of normalized luciferase activity. Luciferase assays were performed by using Dual Luciferase Reporter Gene Assay Kit (Beyotime Biotech. Institute) according to the manufacturer's instructions and results were expressed as the ratio of luciferase to pRL-TK (mean ± S.E.M.).

2.5. Nitric oxide measurement

NO production in live macrophages was detected with the fluorescent probe DAF-FM DA (Invitrogen) by confocal microscopy at excitation/emission maxima of 495/515 nm. Once inside the cells, it is deacetylate by intracellular esterases to become DAF-FM. DAF-FM is essentially non-fluorescent until it reacts with NO. The fluorescence emission intensities of the DAF-FM-stained macrophages (1×10^5/well) were measured by a 96-well plate reader.

Extracellular NO production secretions by macrophages under different treatments in the supernatants were monitored by Griess assay (Promega) according to the manufacturer's instructions.

2.6. iNOS activity assay

We measured iNOS activity by using the Nitric Oxide Synthase Assay Kit (Beyotime). Macrophage-like cells were preincubated with ACs (ratio 1:5) or with CM for 12 h. Then cells were washed twice with PBS so that only the adherent macrophages were retained for iNOS activity assay. The test was performed according to the manufacturer's instructions.

2.7. Laser confocal scanning microscopy (LCSM) and fluorescence resonance energy transfer (FRET) analysis

FRET was used to detect the interaction between GFP-MyD88/CFP-TLR2 and YFP-p85α. Fluorescent emissions from CFP, GFP, YFP, and DAF-FM were measured with LCSM (Zeiss, Jena, Germany), using different excitation wavelengths and detection filters as previously described [19,20].

2.8. Western blot analysis

Cells were lysed with lysis buffer (50 mM Tris–HCl [pH8.0], 150 mM NaCl, 1% TritonX-100, 100 μg/ml PMSF and Protease Inhibitor Cocktail Set I) for 45 min on ice; the fractionation of membranes was prepared using a plasma membrane protein extraction kit according to the instructions of the manufacturer (BioVision, Mountain View, CA). After centrifugation, the expressions of iNOS, HSP70 and β-actin in resulting lysates were analyzed by western blotting [19].

2.9. Statistics

Data are representative of at least three independent experiments and are expressed as mean ± S.E.M. Significant differences

between groups were compared using the one-way ANOVA procedure followed by Student's *t* tests by SPSS software and differences were considered statistically significant at $P < 0.05$.

3. Results

3.1. AC-induced NO production in macrophages

To study the intracellular NO generation triggered by AC, macrophages were stained by DAF-FM DA to fluorescently label NO. RAW264.7 cells showed a dramatic increase of DAF-FM fluorescence emission after 10 h AC (with cultured medium) treatment (Fig. 1A). 1 μg/ml LPS was used as positive controls, and NC was also used as comparison.

To further determine the AC stimulation, we examined NO production in macrophages stimulated either by separated AC or AC conditioned medium (CM). The results indicated that AC, but not any other factors released by AC in CM, induced NO production in macrophages (Fig. 1B). Similar results were also obtained following Griess assay (Fig. 1C). This observation was further supported by western blot analysis of iNOS in RAW264.7 cells (Fig. 1D).

To investigate the kinetics of NO accumulation, time-lapse confocal microscopy was used to observe fluorescence emissions from both macrophage-like cells and primary macrophages after AC treatment. It is clearly showed that AC markedly increased NO production in both types of macrophages (Fig. 1E and F).

3.2. Characterization of contributing factors in AC-induced NO production

Next we sought to characterize the AC-derived unknown factors on macrophages NO formation. To examine the involvement of proteins, we boiled AC for 1 h at 100 °C (AC/100 °C). The heat-inactivated proteins failed to induce NO production, indicating that an unknown protein factor of ACs contributes to NO formation in macrophages. To determine the influence of the lipid factors, we performed chloroform methanol extractions (chloroform/methanol; 2:1) of AC ($CHCl_3$). To completely extract chloroform methanol, PDT-induced AC were broken by repeated freeze–thaw cycles, then the fragments of AC were followed by chloroform methanol extractions (BrO $CHCl_3$). The organic phase was evaporated, reconstituted in PBS containing 1 mg/ml BSA, and added back to macrophages. Both extraction results showed that the lipid fraction of ACs did not induce NO production (Fig. 2A). The results using just freeze/thawed tumor cells (without PDT) showed that the reduction of NO production was not caused by the NC due to heating. To verify the functional importance of HSP70 in the

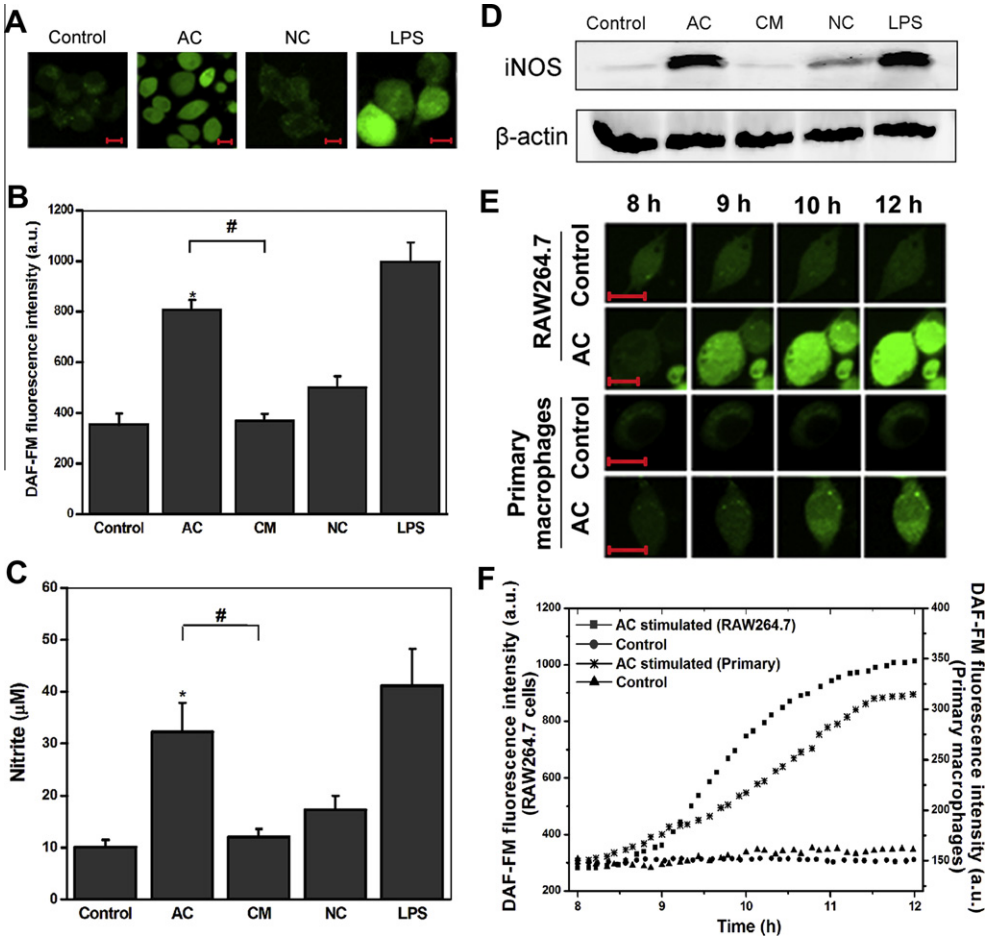

Fig. 1. AC-induced NO production in macrophages. (A) Fluorescent images of DAF-FM in macrophages. The representative images of macrophages were observed using confocal microscope. Bar, 10 μm. (B) and (C) Fluorescence emission intensities of DAF-FM in macrophages measured with 96-well plate reader (B) and extracellular NO production detected by Griess assay (C). Data represent mean ± S.E.M. ($n = 5$; $^{*}P < 0.05$ vs. control cells; $^{\#}P < 0.05$ vs. indicated cells). (D) Representative western blot analysis of macrophages received different treatments to detect iNOS. (E) Representative time lapse fluorescent images of DAF-FM in both RAW264.7 cells (top panel) and primary macrophages (bottom panel). Results represent one of five replicates. Bar, 10 μm. (F) Time lapse fluorescence emission intensities of DAF-FM in macrophages corresponding to the images in E.

process of NO formation in macrophages, we used anti-HSP70-neutralizing antibody to block HSP70 in AC (anti-HSP70), or HSP70 overexpressed EMT6 for PDT (HSP70-AC). Similar to AC/100 °C and the extractions results, the antibody neutralized ACs failed to induce NO production in macrophage-like cells compared with control group. Moreover, ACs overexpressing HSP70 induced a markedly NO formation in macrophages (Fig. 2A). These results were further confirmed by western blot analysis of iNOS (Fig. 2B and C). We also performed HSP70 western blot analysis to confirm the translocation of HSP70 onto AC or HSP70-overexpressed AC cells' surface after PDT treatment (Fig. 2D). Thus, we conclude that after PDT translocation of HSP70 onto cell surface is responsible for NO formation in macrophages.

3.3. Effects of HSP70 on AC-induced macrophage activation

We adopted the RNA interference technique to investigate the role of HSP70 in activated macrophage induced by AC (Fig. 3A). Knockdown of HSP70 by shRNA significantly suppressed AC-induced NO production at 30 min or 10 h (Fig. 3B).

To determine the effects of macrophage phagocytosis on NO formation, we used cytochalasin B (Cyt B) to block phagocytosis. The results showed that unlike shRNA knockdown of HSP70, the phagocytosis-blocking agent Cyt B did not change NO formation at 30 min after AC treatment, while Cyt B significantly decreased NO production at 10 h. Both HSP70 knockdown in AC and macrophage phagocytosis blockage clearly decreased NO production at 30 min and10 h (Fig. 3B). These experimental results indicate that NO production was initially induced by HSP70 on the AC surface, and was further enhanced by macrophage phagocytosis.

3.4. Relationship of iNOS activity and NF-κB with HSP70 in macrophages after AC treatment

To further clarify the relationship of HSP70 and macrophage phagocytosis with NO production in macrophages after AC treat-

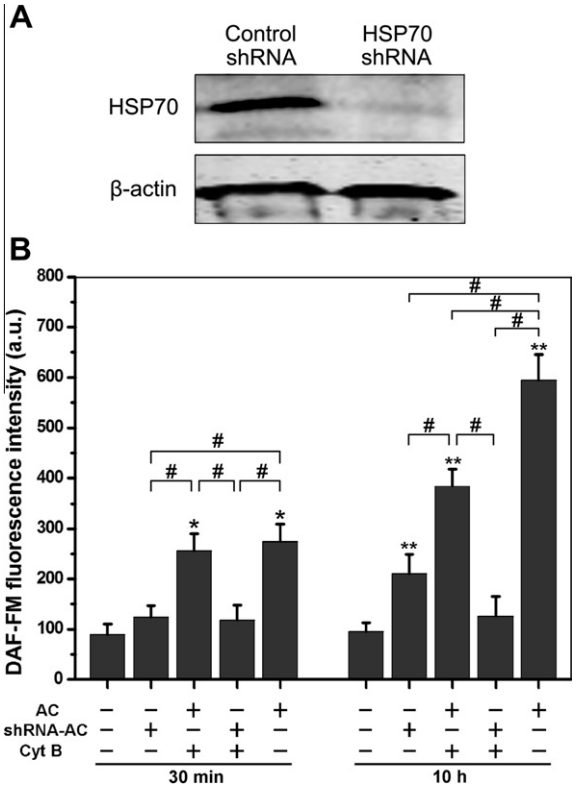

Fig. 3. Effects of HSP70 on AC-induced macrophage activation. (A and B) EMT6 cells were transfected with either specific HSP70 shRNA or non-targeting shRNA. G418-resistant cells were collected for western blot analysis and macrophages stimulation. (A) Representative western blot of HSP70 in EMT6 cells transfected with shRNA; (B) DAF-FM fluorescence intensity from macrophages pretreated with cytochalasin B. NO production in AC or HSP70-blocked AC treated macrophage-like cells were detected by a 96-well plate reader at the indicated times. ($n = 6$; $^{*}P < 0.05$ and $^{**}P < 0.05$ vs. corresponding control cells; $^{\#}P < 0.05$ vs. indicated cells).

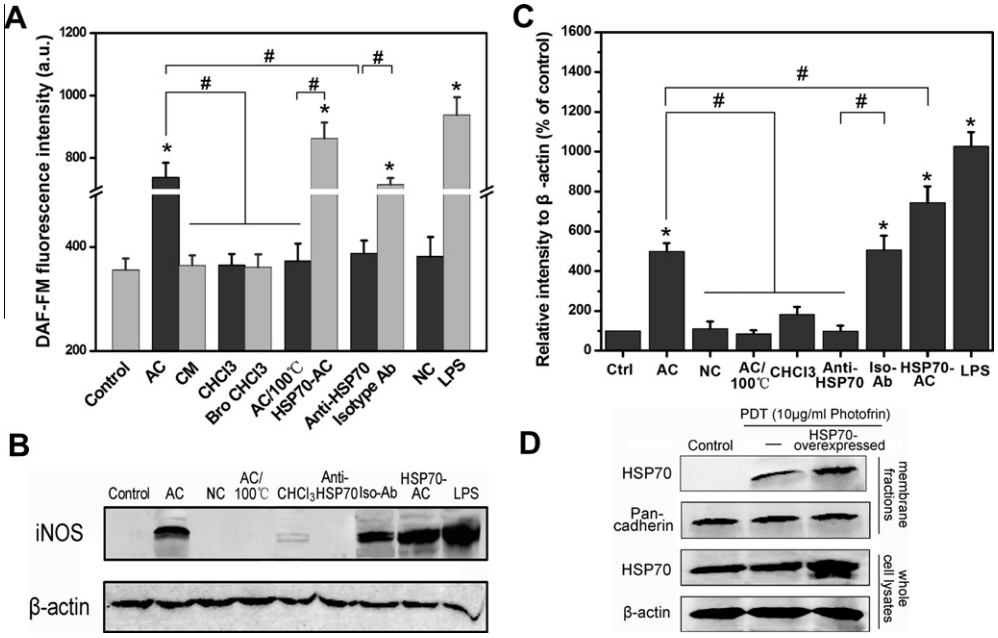

Fig. 2. Characterization of contributing factors in AC-induced NO production. (A) NO production in macrophages induced by different components of AC. Ten hours after stimulation, macrophages were stained with DAF-FM DA and then fluorescence emission intensities were detected by a 96-well plate reader. ($n = 12$; $^{*}P < 0.05$ vs. control cells; $^{\#}P < 0.05$ vs. indicated cells). (B) Different components of AC-induced iNOS expression in macrophages. Representative western blot of iNOS protein was detected. (C) The relative iNOS protein expression was quantified using ImageJ software. ($n = 5$; $^{*}P < 0.05$ vs. control cells; $^{\#}P < 0.05$ vs. indicated cells). (D) Representative western blot analysis of AC cells received different treatments to detect total HSP70 and cell membrane HSP70. AC/100 °C, heat-inactivated protein of AC; $CHCl_3$, lipid fraction of ACs.

ment, iNOS activity assay was performed. It's clearly evident that iNOS activity was mainly induced by HSP70 at 30 min, and that the activity level slowly increased thereafter (Fig. 4A). Knockdown of HSP70 expression in AC significantly suppressed iNOS activity in macrophages at 30 min or 10 h. After blocking macrophage phagocytosis, iNOS activity did not increase from 30 min onwards to 10 h.

Since NF-κB is a key gene transcription factor activated by TLR2 signaling and associated with the expression of pro-inflammatory genes, we performed iNOS and NF-κB reporter analysis as described in Materials and Methods. Either NF-κB- or iNOS-dependent gene reporter assay revealed that AC had an increased effect on NF-κB and iNOS transactivation activity in macrophages (Fig. 4A). However, macrophages treated with HSP70-blocked AC or pretreated with Cyt B then stimulated with AC both failed to induce an increase of such transactivation activity after 10 h stimulation, suggesting that HSP70-induced macrophage phagocytosis play an important role in NF-κB-mediated iNOS expression (Fig. 4B).

3.5. Effects of MyD88 and PI3K on NO production

To further determine the involvement of TLRs in AC-induced macrophage activation, we measured NO production and iNOS activity in mouse primary macrophages. It is clearly evident, as shown in Fig. 5A and B, that the dominant negative form of MyD88 (DN MyD88) markedly suppressed both NO production and iNOS activity in macrophages after 10 h AC treatment. Studies have shown that regulation of iNOS activation is involved in the activation of PI3K signaling, which either serves as a negative regulation or positive regulation of iNOS activation [21,22]. We further determined the effects of PI3K on NO production and iNOS activity in mouse primary macrophages. The results show that both Δp85α (dominant negative form of the regulatory subunit of PI3K) and wortmannin reduced NO production and iNOS activity. Consistent with the results in Fig. 2, the anti-HSP70 neutralized AC significantly inhibited the NO production and iNOS activity. These results clearly show that the adaptor molecule MyD88 and the PI3 K signal transduction pathway triggered by ACs lead to the activation of iNOS, which are further confirmed by western blot analysis of iNOS (Fig. 5C and D).

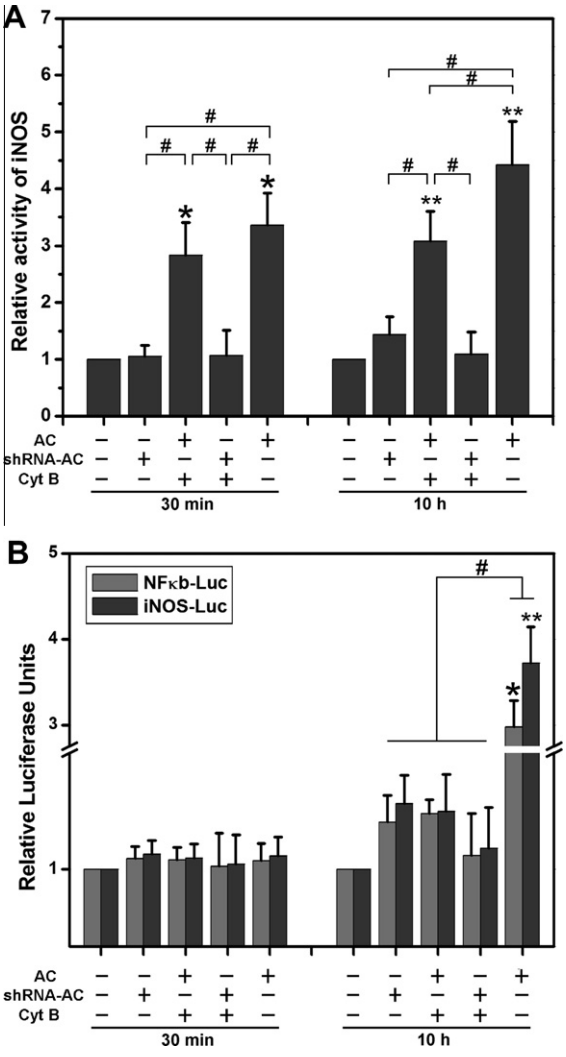

Fig. 4. Relationship between iNOS activity and NF-κB with HSP70 in macrophages after AC treatment. Cells were treated as described in Fig. 3 legend. (A) Relative activity of iNOS in macrophage-like cells. ($n = 6$; $^{*}P < 0.05$ and $^{**}P < 0.05$ vs. corresponding control cells; $^{\#}P < 0.05$ vs. indicated cells). (B) Relative luciferase activity in macrophage-like cells. ($n = 6$; $^{*}P < 0.05$ and $^{**}P < 0.05$ vs. corresponding control cells; $^{\#}P < 0.05$ vs. indicated cells).

3.6. Relationship between TLR2, MyD88 and PI3K activation in macrophage during AC stimulation

We have demonstrated that HSP70 is quickly expressed on the cell surface under PDT-induced apoptosis, and presents potent endogenous danger signals to macrophages through TLR2 [14]. To further explore TLR2-mediated signal-transduction pathway, we adopted the FRET technique to investigate PI3 K activation induced by PDT-treated AC. Macrophage-like cells were co-transfected with YFP-p85α and GFP-MyD88, and then the real-time GFP, FRET, and FRET/GFP fluorescence images were collected with LCSM. The results showed that the interaction of p85α and MyD88 increased during AC-induced macrophage activation (Fig. 6B).

We also found that blocking PI3K was more efficiency than blocking MyD88 on both NO production and iNOS activity (Fig. 5). It appears that PDT-induced AC activates PI3K in macrophages before MyD88 activation.

To validate the results shown in Fig. 5, macrophage-like cells were co-transfected with CFP-TLR2 and YFP-p85α. The results showed that TLR2 directly interacted with p85α in AC stimulated macrophage-like cells (Fig. 6C and D). We transfected macrophage-like cells with DN TLR2 to further confirm whether TLR2 was responsible for the observed effects. The results show that DN TLR2 significantly suppressed AC-induced NO production in macrophages (Fig. 6E). These experimental results show TLR2-mediated NO production undergoing both dependent and independent MyD88 signal transduction pathways in macrophage-like cells.

4. Discussion

The immune response induced by AC, either immunostimulatory or immunosuppressive, have been extensively studied. However, the molecular mechanisms of the immunostimulatory effects induced by PDT-treated AC remain unclear. In this study, we investigated the molecular mechanism of macrophage activation by PDT-induced AC. We demonstrated that PDT-treated ACs were capable of stimulating NO production in macrophages (Fig. 1), consistent with AC's ability to increase iNOS activity and up-regulate NF-κB-dependent iNOS expression (Fig. 4D).

Mammalian systems contain three well-characterized isoforms of NOS: iNOS, eNOS, and nNOS. Altered NO production, produced by iNOS, have been linked to the pathogenesis of various biological and inflammatory disorders [23]. Thus, understanding cellular processes responsible for controlling NO production by iNOS is critical for designing and developing therapeutic strategies for immunomodulation associated with iNOS production and/or activity.

Although the immunostimulatory role of AC and NC is apparent, the mechanism of AC-induced NO secretion from macrophages is

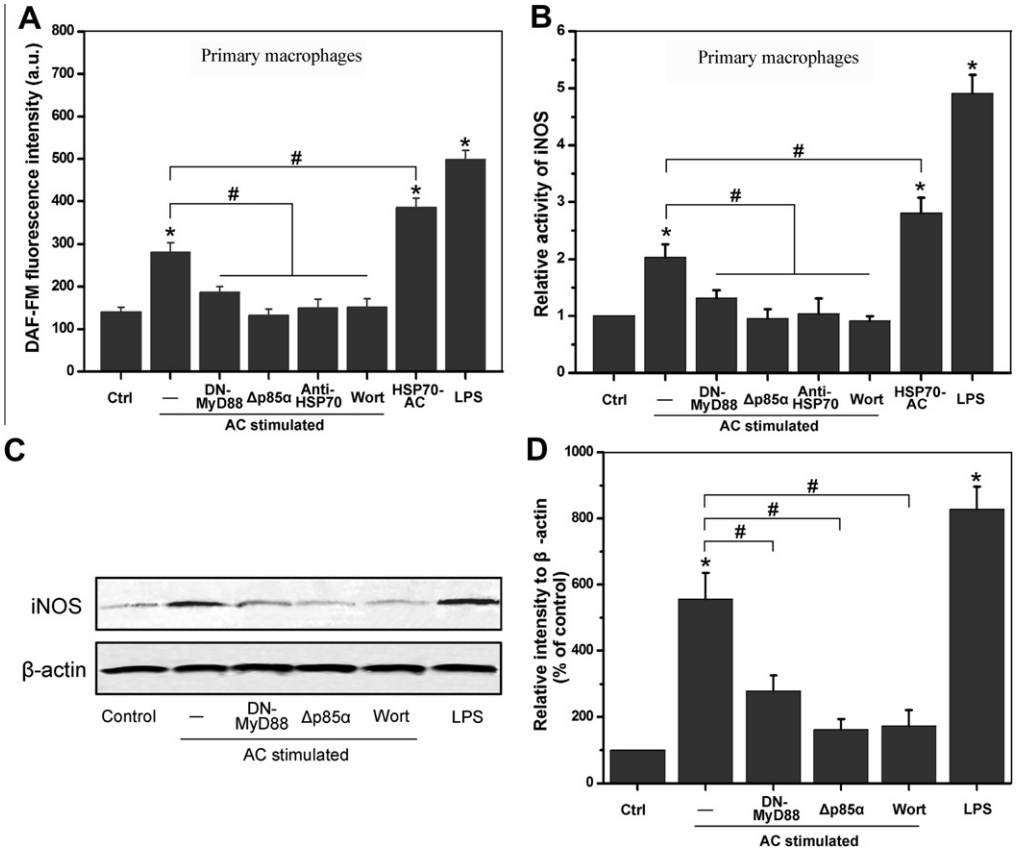

Fig. 5. Effects of MyD88 and PI3K on AC-induced NO production in macrophages. (A) and (B) DAF-FM fluorescence intensity and relative activity of iNOS. Primary macrophages pretreated with wortmannin or transfected with DN MyD88 or Δp85α, and G418-resistant cells were collected for further treatments. Macrophages were incubated with AC, HSP70-AC or anti-HSP70-neutralized AC for 10 h; both NO production (A) and iNOS activity were measured (B). Data represent mean ± S.E.M. ($n = 12$; $^{*}P < 0.05$ vs. control cells; $^{\#}P < 0.05$ vs. indicated cells). (C) Representative western blots of iNOS expression in macrophages; (D) The relative iNOS protein expression was quantified using ImageJ software. ($n = 5$; $^{*}P < 0.05$ vs. control cells; $^{\#}P < 0.05$ vs. indicated cells).

not fully understood. Various peptides or cytokines expressed by AC have been shown to induce immune responses [24]. To date, we have not identified all the potential bioactive components that activate macrophages in PDT-induced AC conditioned medium. The influence of protein was determined based on the use of heat-inactivated AC, which attenuated AC-induced NO production in our system (Fig. 2). Since cytoplasmic HSP70 could translocate onto the cell surface after PDT treatment [25,26], neutralization of HSP70 blocked AC-induced expression of NO production in macrophages. These results suggest that the translocated HSP70 from AC, which is responsible for the upregulation of iNOS expression in macrophages. Our results further indicated that NO production was initially induced by HSP70 on the AC surface, and was further enhanced by macrophage phagocytosis (Fig. 3).

In macrophages, iNOS expression was NF-κB dependent [27]. Indeed, we have shown that AC had an increased effect on iNOS activity and NF-κB-/iNOS-derived luciferase activity in macrophages (Fig. 4). Furthermore, we showed that PDT-induced AC could activate PI3K transduction signal. Both wortmannin and Δp85α reduced NO production and iNOS activity in mouse primary macrophages (Fig. 5A and B). Although some studies showed that PI3K had a negative impact on NO production in macrophages [21], our results showed that PI3K was required in macrophages NO formation, which was further confirmed by western blot analysis of iNOS (Fig. 5C and D). Additionally, we verified that the activation of PI3K was directly involved in the interaction between MyD88 and p85α (Fig. 6A and B).

All TLRs are believed to be dependent on signalling through the MyD88, which is known as an immediate downstream adaptor molecule that interacts directly with the TIR domain of TLRs [28], except for TLR3 [29]. Our results also demonstrated that PDT-induced AC activated macrophages depending on TLR2 (Fig. 6) and MyD88 (Fig. 5). Although there are many other contributors responsible for NO formation, our experimental results suggest that MyD88 and PI3K are primary participants in NO signalling pathway. We also found that blocking PI3K was more efficient than blocking MyD88 in both NO production and iNOS activity. It is likely that AC-induced TLRs-mediated NO production in macrophages is through a MyD88-independent pathway.

Hence, we extended this observation by demonstrating that the direct interaction between TLR2 and p85α was induced by AC (Fig. 6C and D). These results suggest that PDT-treated AC provides a TLR2 dependent signal to activate the formation of NO in macrophages, either via TLR2-MyD88-PI3K or TLR2-PI3K pathway. One of the most plausible explanations of the results is that TLR2 contains a consensus-binding motif (YXXM) for the p85α, which is distinctive from the binding site for MyD88 [30]. Unlike TLR4, TLR2 and MyD88 both have a binding motif for p85α. Since MyD88 is not only involved in the signaling process of multiple TLRs, but also in the signaling process after activation of members of the IL-1 receptor family, the role of TLR2 on the observed effects was further confirmed by using DN TLR2 (Fig. 6E).

It is well established that formation of iNOS protein dimers is essential for sustained enzymatic activity [31]. Kouhei Sakai et al. have demonstrated that PI3K is important in dimerization of iNOS protein and thus crucial in NO production and the innate immune response [22]. In addition, a recent study showed that TLR2–MyD88-dependent signaling enhanced macrophages phagocytosis

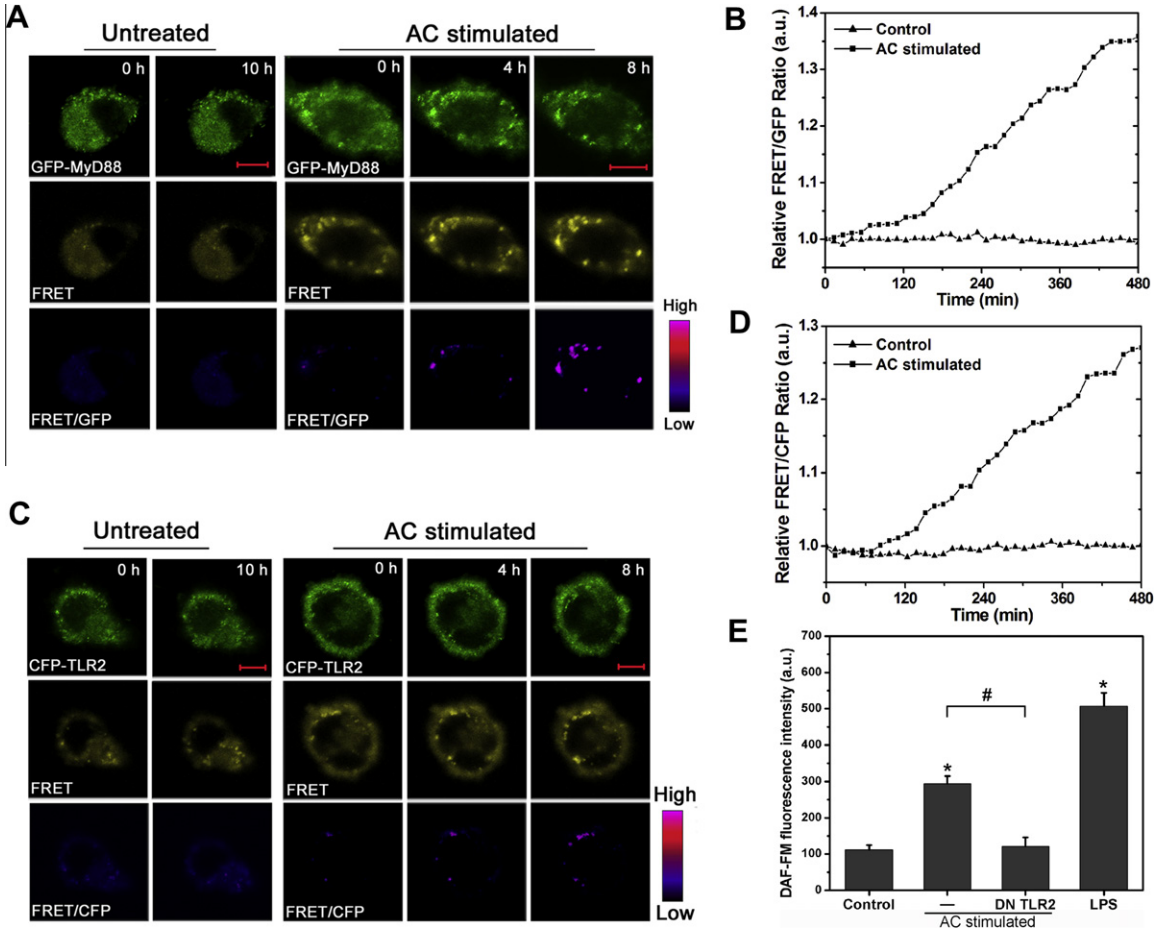

Fig. 6. Direct interaction between TLR2, MyD88 and PI3K. (A) Representative fluorescence images in control macrophages (left panel) and in AC treated macrophages (right panel) in GFP-channel, FRET-channel and FRET/GFP ratio-channel. The images of FRET/GFP ratio were processed with pseudocolor technique. Bar, 10 μm. (B) Quantitative analysis of FRET/GFP ratio corresponding to the images in (A), with the FRET/GFP ratio normalized to 1. Results represent one of five replicates. (C) Representative fluorescence image series of CFP, FRET, and FRET/CFP in control (left panel) and AC treated CFP-TLR2 and YFP-p85α cotransfected macrophages (right panel). The images of FRET/CFP ratio were processed with pseudocolor technique. Bar, 10 μm. (D) Quantitative analysis of FRET/CFP ratio corresponding to the images in C. The FRET/CFP ratio is normalized to 1. Results represent one of five replicates. (E) RAW264.7 cells transfected with DN TLR2 and G418-resistant cells were collected for AC treatments, then NO production were measured. Data represent mean ± S.E.M. ($n = 6$; $^{*}P < 0.05$ vs. control cells; $^{\#}P < 0.05$ vs. indicated cells).

through activation of PI3K and Rac1 [32]. It seems that PI3K plays a key role in cross-talk between iNOS enzyme activity and phagocytosis in macrophages. In our study, the HSP70 on the AC surface is believed to be responsible for the iNOS enzyme activity through quick activation of PI3K, while macrophage phagocytosis of AC is responsible for upregulating NF-κB-dependent iNOS expression. This supposition is consistent with the results in Fig. 4.

In summary, we report for the first time that the HSP70-induced NO production in macrophages is mediated via TLR2 signal transduction pathway and that TLR2 utilizes both MyD88-dependent and -independent pathways to transduce its signal. Here, HSP70 translocated onto cell surface rather than released into the culture supernatants in PDT-treated cells during apoptosis, indicating that AC but not other AC-released factors induced NO formation. More importantly, this study provides a feasible molecular mechanism of PDT-mediated immune response, involving NO production of macrophages, a result from activation of iNOS enzyme activity with the combination of activation of transcriptional factor NF-κB. Therefore, these results provide an important clue to elucidate the molecular mechanisms linking innate immune signalling to apoptosis by which PDT-treated AC induce macrophages activation and the consequent cellular responses through the TLR2, laying the foundation for further understanding of immunostimulatory mechanism of PDT and paving the way for future development of highly effective PDT treatment.

Conflict of interest

The authors declare no financial or commercial conflict of interest.

Acknowledgements

This research is supported by the National Basic Research Program of China (2011CB910402; 2010CB732602), the Program for Changjiang Scholars and Innovative Research Team in University (IRT0829), and the National Natural Science Foundation of China (81101741).

We are grateful to acknowledge specifically those who have been listed in Materials and method for help with plasmids.

References

[1] Pinkoski, M.J. and Green, D.R. (2005) Apoptosis in the regulation of immune responses. J. Rheumatol. Suppl. 74, 19–25.
[2] Peng, Y., Martin, D.A., Kenkel, J., Zhang, K., Ogden, C.A. and Elkon, K.B. (2007) Innate and adaptive immune response to apoptotic cells. J. Autoimmun. 29, 303–309.
[3] Torchinsky, M.B., Garaude, J., Martin, A.P. and Blander, J.M. (2009) Innate immune recognition of infected apoptotic cells directs T(H)17 cell differentiation. Nature 458, 78–82.
[4] Agostinis, P. et al. (2011) Photodynamic therapy of cancer: an update. CA Cancer J. Clin. 61, 250–281.

[5] Korbelik, M. and Dougherty, G.J. (1999) Photodynamic therapy-mediated immune response against subcutaneous mouse tumors. Cancer Res. 59, 1941–1946.
[6] Castano, A.P., Mroz, P. and Hamblin, M.R. (2006) Photodynamic therapy and anti-tumour immunity. Nat. Rev. Cancer 6, 535–545.
[7] Castano, A.P., Mroz, P., Wu, M.X. and Hamblin, M.R. (2008) Photodynamic therapy plus low-dose cyclophosphamide generates antitumor immunity in a mouse model. Proc. Natl. Acad. Sci. USA 105, 5495–5500.
[8] Demidova, T.N. and Hamblin, M.R. (2004) Macrophage-targeted photodynamic therapy. Int. J. Immunopathol. Pharmacol. 17, 117–126.
[9] Ho, V.W. and Sly, L.M. (2009) Derivation and characterization of murine alternatively activated (M2) macrophages. Methods Mol. Biol. 531, 173–185.
[10] Korbelik, M., Naraparaju, V. and Yamamoto, N. (1997) Macrophage-directed immunotherapy as adjuvant to photodynamic therapy of cancer. Br. J. Cancer 75, 202.
[11] Korbelik, M. (2009) Complement upregulation in photodynamic therapy-treated tumors: role of Toll-like receptor pathway and NFkappaB. Cancer Lett. 281, 232–238.
[12] Martin-Manso, G., Galli, S., Ridnour, L.A., Tsokos, M., Wink, D.A. and Roberts, D.D. (2008) Thrombospondin 1 promotes tumor macrophage recruitment and enhances tumor cell cytotoxicity of differentiated U937 cells. Cancer Res. 68, 7090–7099.
[13] Scheffer, S.R., Nave, H., Korangy, F., Schlote, K., Pabst, R., Jaffee, E.M., Manns, M.P. and Greten, T.F. (2003) Apoptotic, but not necrotic, tumor cell vaccines induce a potent immune response in vivo. Int. J. Cancer 103, 205–211.
[14] Zhou, F., Xing, D. and Chen, W.R. (2009) Regulation of HSP70 on activating macrophages using PDT-induced apoptotic cells. Int. J. Cancer 125, 1380–1389.
[15] Garg, A.D. et al. (2012) A novel pathway combining calreticulin exposure and ATP secretion in immunogenic cancer cell death. EMBO J. 31, 1062–1079.
[16] Ruttimann, J. (2007) Macrophages and nitric oxide: a deadly combination. J. Exp. Med. 204, 3057.
[17] Sanzen, I. et al. (2001) Nitric oxide-mediated antitumor activity induced by the extract from Grifola frondosa (Maitake mushroom) in a macrophage cell line, RAW264.7. J. Exp. Clin. Cancer Res. 20, 591–597.
[18] Zhou, F., Xing, D. and Chen, W.R. (2008) Dynamics and mechanism of HSP70 translocation induced by photodynamic therapy treatment. Cancer Lett. 264, 135–144.
[19] Li, H., Liu, L., Xing, D. and Chen, W.R. (2010) Inhibition of the JNK/Bim pathway by Hsp70 prevents Bax activation in UV-induced apoptosis. FEBS Lett. 584, 4672–4678.
[20] Wang, X., Xing, D., Liu, L. and Chen, W.R. (2009) BimL directly neutralizes Bcl-xL to promote Bax activation during UV-induced apoptosis. FEBS Lett. 583, 1873–1879.
[21] Diaz-Guerra, M.J., Castrillo, A., Martin-Sanz, P. and Bosca, L. (1999) Negative regulation by phosphatidylinositol 3-kinase of inducible nitric oxide synthase expression in macrophages. J. Immunol. 162, 6184–6190.
[22] Sakai, K. et al. (2006) Phosphoinositide 3-kinase in nitric oxide synthesis in macrophage: critical dimerization of inducible nitric-oxide synthase. J. Biol. Chem. 281, 17736–17742.
[23] Szabo, C., Salzman, A.L. and Ischiropoulos, H. (1995) Endotoxin triggers the expression of an inducible isoform of nitric oxide synthase and the formation of peroxynitrite in the rat aorta in vivo. FEBS Lett. 363, 235–238.
[24] Gardai, S.J., Bratton, D.L., Ogden, C.A. and Henson, P.M. (2006) Recognition ligands on apoptotic cells: a perspective. J. Leukoc. Biol. 79, 896–903.
[25] Korbelik, M., Sun, J. and Cecic, I. (2005) Photodynamic therapy-induced cell surface expression and release of heat shock proteins: relevance for tumor response. Cancer Res. 65, 1018–1026.
[26] Merchant, S. and Korbelik, M. (2011) Heat shock protein 70 is acute phase reactant: response elicited by tumor treatment with photodynamic therapy. Cell Stress Chaperones 16, 153–162.
[27] Subbanagounder, G., Wong, J.W., Lee, H., Faull, K.F., Miller, E., Witztum, J.L. and Berliner, J.A. (2002) Epoxyisoprostane and epoxycyclopentenone phospholipids regulate monocyte chemotactic protein-1 and interleukin-8 synthesis. Formation of these oxidized phospholipids in response to interleukin-1beta. J. Biol. Chem. 277, 7271–7281.
[28] Burns, K. et al. (1998) MyD88, an adapter protein involved in interleukin-1 signaling. J. Biol. Chem. 273, 12203–12209.
[29] Akira, S. and Takeda, K. (2004) Toll-like receptor signalling. Nat. Rev. Immunol. 4, 499–511.
[30] Cantley, L.C. (2002) The phosphoinositide 3-kinase pathway. Science 296, 1655–1657.
[31] Baek, K.J., Thiel, B.A., Lucas, S. and Stuehr, D.J. (1993) Macrophage nitric oxide synthase subunits. Purification, characterization, and role of prosthetic groups and substrate in regulating their association into a dimeric enzyme. J. Biol. Chem. 268, 21120–21129.
[32] Shen, Y. et al. (2010) Toll-like receptor 2- and MyD88-dependent phosphatidylinositol 3-kinase and Rac1 activation facilitates the phagocytosis of Listeria monocytogenes by murine macrophages. Infect. Immun. 78, 2857–2867.